Pflügers Archiv - European Journal of Physiology (2019) 471:365–380
https://doi.org/10.1007/s00424-018-2212-2

SIGNALING AND CELL PHYSIOLOGY

Carbocisteine stimulated an increase in ciliary bend angle via a decrease in $[Cl^-]_i$ in mouse airway cilia

Yukiko Ikeuchi[1,2] · Haruka Kogiso[1,2] · Shigekuni Hosogi[1] · Saori Tanaka[3] · Chikao Shimamoto[3] · Hitoshi Matsumura[3] · Toshio Inui[2,4] · Yoshinori Marunaka[1,2,5] · Takashi Nakahari[2]

Received: 2 June 2018 / Revised: 24 August 2018 / Accepted: 25 September 2018 / Published online: 6 October 2018

Abstract

Carbocisteine (CCis), a mucoactive agent, is widely used to improve respiratory diseases. This study demonstrated that CCis increases ciliary bend angle (CBA) by 30% and ciliary beat frequency (CBF) by 10% in mouse airway ciliary cells. These increases were induced by an elevation in intracellular pH (pH_i; the pH_i pathway) and a decrease in the intracellular Cl^- concentration ($[Cl^-]_i$; the Cl^- pathway) stimulated by CCis. The Cl^- pathway, which is independent of CO_2/HCO_3^-, increased CBA by 20%. This pathway activated Cl^- release via activation of Cl^- channels, leading to a decrease in $[Cl^-]_i$, and was inhibited by Cl^- channel blockers (5-nitro-2-(3-phenylpropylamino) benzoic acid and CFTR(inh)-172). Under the CO_2/HCO_3^--free condition, the CBA increase stimulated by CCis was mimicked by the Cl^--free NO_3^- solution. The pH_i pathway, which depends on CO_2/HCO_3^-, increased CBF and CBA by 10%. This pathway activated HCO_3^- entry via Na^+/HCO_3^- cotransport (NBC), leading to a pH_i elevation, and was inhibited by 4,4′-diisothiocyano-2,2′-stilbenedisulfonic acid. The effects of CCis were not affected by a protein kinase A inhibitor (1 μM PKI-A) or Ca^{2+}-free solution. Thus, CCis decreased $[Cl^-]_i$ via activation of Cl^- channels including CFTR, increasing CBA by 20%, and elevated pH_i via NBC activation, increasing CBF and CBA by 10%.

Keywords Airway cilia · Intracellular Cl^- concentration · Ciliary beating angle · Inner dynein

Introduction

Mucociliary clearance is a host-defense mechanism of the lungs and involves the mucous layer and the beating cilia lining the airway surface. The surface mucous layer entraps inhaled small particles, including dust, bacteria, and viruses, and is swept towards the oropharynx by the beating cilia [1, 37, 48]. Thus, mucociliary transport is compared to a belt conveyer system for removing inhaled particles from the airway [11], in which the beating cilia are the engine. Therefore, drugs stimulating ciliary beating are of particular importance to improve respiratory diseases.

Ciliary beating is activated by many substances, including cyclic adenosine monophosphate (cAMP), Ca^{2+}, ATP, and β_2-agonists [22–24, 37, 38, 48], and modulated by cellular events, such as cell shrinkage, $[Cl^-]_i$ decrease [38, 45], and changes in intracellular pH (pH_i) [42]. Carbocisteine (CCis), a mucoactive agent used for the treatment of respiratory diseases, is thought to activate mucociliary clearance [18, 36] based on the following observations. CCis stimulates Cl^- secretion in tracheal epithelia via anion channels including cystic fibrosis transmembrane conductance regulator (CFTR) [12, 30], which also plays crucial roles in HCO_3^- secretion [5, 21]. These observations suggest that CCis may stimulate ciliary beatings mediated via changes in cell volume and pH_i coupled with anion transport, especially HCO_3^- transport, in airway ciliary cells. However, the effects of CCis on beating cilia in the airways remain uncertain [18, 33, 36].

✉ Takashi Nakahari
nakahari@fc.ritsumei.ac.jp

1 Department of Molecular Cell Physiology, Graduate School of Medical Science, Kyoto Prefectural University of Medicine, Kyoto 602-8566, Japan

2 Research Center for Drug Discovery and Pharmaceutical Development Science, Research Organization of Science and Technology, BKC, Ritsumeikan University, 1-1-1 Nojihigashi, Kusatsu, Shiga 525-8577, Japan

3 Laboratory of Pharmacotherapy, Osaka University of Pharmaceutical Sciences, Takatsuki, Japan

4 Saisei Mirai Clinics, Moriguchi 570-0012, Japan

5 Research Institute for Clinical Physiology, Kyoto Industrial Health Association, Kyoto 604-8472, Japan

Ciliary beating activities can be assessed by two parameters, ciliary beat frequency (CBF) and ciliary bend angle (CBA, an index of ciliary bend amplitude) [22–24]. Previous studies in *Chlamydomonas* showed that axonemal beating is driven by two functionally distinct dyneins (molecular motors), namely, the inner dynein arm (IDA) and the outer dynein arm (ODA) [6, 7]. *Chlamydomonas* mutant studies revealed that IDAs change the waveform, including the amplitude (CBA), and ODAs change the frequency (CBF) [6].

In this study, we examined the effects of CCis on CBA and CBF in isolated airway ciliary cells using a video microscope equipped with a high-speed camera [22–24]. CCis stimulated an increase in CBA and CBF, which coincided with a $[Cl^-]_i$ decrease in airway ciliary cells. As a decrease in $[Cl^-]_i$ has been shown to modulate some cellular functions [28, 29], this decrease may be an essential signal to increase the CBA and CBF of airway cilia during CCis stimulation. The aim of this study is to confirm this hypothesis.

Materials and methods

Solution and chemicals

The control solution contained the following (in mM): NaCl, 121; KCl, 4.5; $NaHCO_3$, 25; $MgCl_2$, 1; $CaCl_2$, 1.5; Na-HEPES, 5; H-HEPES, 5; and glucose, 5. For preparation of the CO_2/HCO_3^--free solution, $NaHCO_3$ was replaced with NaCl, and for preparation of the Cl^--free solution, Cl^- was replaced with NO_3^-. The CO_2/HCO_3^--containing solutions were aerated with 95% O_2 and 5% CO_2, and the CO_2/HCO_3^--free solutions were aerated with 100% O_2. The pH values of the solutions were adjusted to 7.4 by adding 1N-HCl or 1N-HNO_3, as appropriate. The experiments were carried out at 37 °C. 5-Nitro-2-(3-phenylpropylamino) benzoic acid (NPPB), 4-[[4-oxo-2-thioxo-3-[3-(trifluoromethyl)phenyl]-5-thiazolidinylidene]methyl]-benzoic acid (CFTR(inh)-172) and 4,4′-diisothiocyano-2,2′-stilbenedisulfonic acid (DIDS) were purchased from Sigma (St. Louis, MO, USA); carbocisteine (CCis, *S*-(carboxymethyl)-L-cysteine), heparin, elastase, bovine serum albumin (BSA), and dimethyl sulfoxide (DMSO) were from Wako Pure Chemical Industries, Ltd. (Osaka, Japan). CCis was dissolved in 0.1 N HCl, and other reagents were dissolved in DMSO; these solutions were then stored at − 20 °C. All reagents were prepared to their final concentrations immediately before the experiments. The DMSO concentration did not exceed 0.1%, and DMSO at this concentration had no effect on CBF and CBA [22–24, 38].

Cell preparation

The mice were anesthetized with inhaled isoflurane (3%), further anesthetized with an intraperitoneal injection (ip) of pentobarbital sodium (40 mg/kg), and heparinized (1000 units/kg) for 15 min. Then, the mice were sacrificed by a high dose of pentobarbital sodium (100 mg/kg, ip). Cell isolation procedures have already described in details [22–24, 38]. Briefly, after the mice were sacrifices, a thoracotomy was carried out. Then, the lungs were cleared of blood by perfusion via the pulmonary artery, and the lungs, with the trachea and heart, were removed from the animal en bloc. A nominally Ca^{2+}-free solution (0.5 ml) was instilled into the lung cavity via the tracheal cannula and then removed. This procedure was repeated four times. The fifth instillation was retained in the lung cavity for 5 min, and the lung cavity was then washed five times with the control solution via the tracheal cannula. Finally, the control solution containing elastase (0.2 mg/ml) and DNase I (0.02 mg/ml) was instilled into the lung cavity, and the airway epithelium was digested for 40 min at 37 °C. Following this incubation, the lungs were minced using fine forceps in control solution containing DNase I (0.02 mg/ml) and BSA (5%). The minced tissue was filtered through a nylon mesh (a sieve with 300-μm openings). The cells were washed three times with centrifugation (160×*g* for 5 min) and then suspended in the control solution. The cell suspension was stored at 4 °C, and cells were used within 5 h after the isolation.

CBA and CBF measurements

Cells were placed on a coverslip precoated with Cell-Tak (Becton Dickinson Labware, Bedford, MA, USA). Coverslips were set in a micro-perfusion chamber (20 μl) mounted on an inverted light microscope (Eclipse Ti, NIKON, Tokyo, Japan) connected to a high-speed camera (FASTCAM-1024PCI, Photron Ltd., Tokyo, Japan). The stage of the microscope was heated to 37 °C, as CBF is highly dependent on temperature [11]. Cells were perfused at 200 μl/min with the control solution aerated with a gas mixture (95% O_2 and 5% CO_2) at 37 °C. Ciliary cells, which were distinguished from other cells by their beating cilia, accounted for 10–20% of isolated lung cells. For the CBA (angle) and CBF measurements, video images were recorded for 2 s at 500 fps [22–24]. Before the start of the experiments, cells were perfused with control solution for 5 min. After the experiments, CBA and CBF were measured using an image analysis program (DippMotion 2D, Ditect, Tokyo, Japan). The method to measure CBA and CBF has been previously described [22]. The CBA and CBF ratios (CBA_t/CBA_0 and CBF_t/CBF_0), values of which were normalized to the control values, were used to make a comparison among the experiments. The subscript 0 or *t* indicates the time before or after the start of experiments, respectively. Each experiment was carried out using four to ten cover slips with cells obtained from 2 to 5 animals. In each coverslip, we selected one to two cells or a cell block and measured their CBAs and

CBFs. The normalized CBA and CBF (CBA ratio and CBF ratio) calculated from 4 to 12 cells were plotted, and *n* shows the number of cells.

Measurement of the cell volume

For cell volume measurements, the outline of a ciliary cell was traced on a video image, and the area (*A*) was measured. The index of cell volume ($V_t/V_0 = (A_t/A_0)^{1.5}$) was calculated [31]. The indices of cell volume measured every 1 min during the control perfusion (5 min) were averaged, and the averaged value was used as V_0. The subscript 0 or *t* indicates the time before or after the start of experiments, respectively. Each experiment was carried out using four to six cover slips obtained from two to three animals. The V/V_0s calculated from four to six cells were plotted, and *n* shows the number of cells.

Measurement of pH_i and $[Cl^-]_i$

To measure intracellular pH (pH_i) of airway ciliary cells, we used carboxy-SNARF-1 (a pH-sensitive fluorescent dye) [17]. Cells were incubated with 10 μM carboxy SNARF1-AM for 60 min at 37 °C, and the cells were set on the heated stage (37 °C) of an inverted confocal laser microscope (model LSM510 META, Carl Zeiss, Jena, Germany). The excitation wavelength was 515 nm, and the emission wavelengths were 645 and 592 nm. The fluorescence ratio (F645/F592) was calculated. The calibration line was obtained using calibration solutions. The calibration solution containing 110 mM KCl, 25 mM $KHCO_3$, 11 mM glucose, 1 mM $MgCl_2$, 1 mM $CaCl_2$, 10 mM HEPES, and 10 μM nigericin was aerated with 95% air and 5% CO_2. The pH of the calibration solution was adjusted to 6.8, 7.2, 7.4, 7.6, or 7.8 by adding 1 M CsOH at 37 °C. The pH_i of ciliary cells was calculated from the calibration line.

Intracellular chloride concentration ($[Cl^-]_i$) was measured using MQAE (N-Ethoxycarbonylmethyl-6-methoxyquinolinium bromide, a chloride fluorescence dye)-based two photon confocal microscopy [17, 19]. Isolated ciliary cells were incubated with 10 mM MQAE for 60 min at 37 °C. MQAE was excited at 780 nm using a two-photon excitation laser system (MaiTai, Spectra-Physics). The emission was 510 nm. The ratio of fluorescence intensity (F_0/F_t) was calculated. The subscript 0 or *t* indicates the time before or after the start of experiments, respectively.

Antibodies

Mouse monoclonal anti-CFTR, [CF3] ab2784 (clone CF3, originally developed by Per et al. [35], Abcam, Cambridge, UK), was used for CFTR staining. The antibody, ab2784, was used to detect CFTR in human airway adenocarcinoma cell line Calu 3 [34], human tracheal cell line CFT1-LCFSN [35], mouse intestine [2], and sperm flagella in mouse [47, 49] and guinea pig [9]. Rabbit polyclonal anti-ARL13B (ADP-ribosylation factor-like protein 13B), 17711-1-AP (Proteintech, Rosemont, IL, USA), was used for cilia staining, because ARL13B, a small GTPase, is localized in cilia.

Western blot analysis

Western blottings detecting cystic fibrosis transmembrane conductance regulator (CFTR) were carried out using isolated lung cells and striated muscles of thigh. The procedures for protein extraction and western blotting have already been described in the previous reports [23]. The antibodies used were anti-CFTR antibody [CF3] ab2784 (Abcam plc, Cambridge, UK) and goat anti-mouse IgM mu chain (HRP) ab97230 (secondary antibody, 1:10000). The protein band was visualized by an enhanced chemiluminescence reagent (WSE-712 EzWestLumi plus, ATTO Corporation, Tokyo, Japan) and captured by a Lumino-image analyzer (LAS 3000; Fuji Film, Tokyo, Japan).

Immunofluorescence microscopic examination

The immunofluorescence images of isolated ciliary cells were also observed using a confocal laser microscope (model LSM 510META, Carl Zeiss, Jena, Germany) [19, 23]. The isolated lung cells were attached on the coverslip and dried. Then, they were fixed in 4% paraformaldehyde (Nacalai tesque, Kyoto, Japan) for 30 min and dried. After the fixation, they were permeabilized by 0.1% Triton X-100 (Sigma, St. Louis, MO, USA). For the immunofluorescence staining, the samples were incubated with anti-CFTR antibody [CF3] ab2784 and anti-ARL13B 17711-1-AP for 12 h at 4 °C. After this incubation, the samples were incubated with the secondary antibodies for 2 h. The secondary antibodies used were Alexa Fluor 488, goat anti-mouse IgM (heavy chain) cross-adsorbed secondary antibody (1:500; Invitrogen, Carlsbad, CA, USA), and Alexa Fluor 546, goat anti-rabbit IgG (H + L) highly cross-adsorbed secondary antibody (1:250; Invitrogen, Carlsbad, CA, USA). The samples on the coverslip were enclosed with VECTASHIELD HardSet Mounting Medium with DAPI (Vector, Burlingame, CA, USA).

Statistical analysis

Data are expressed as the means ± standard error (SEM). Statistical significance between means was assessed by analysis of variance (ANOVA) or Student's *t* test, as appropriate.

Differences were considered significant at $p < 0.05$. The statistical significance is shown in the figures.

Results

Cellular events activated by CCis

CCis stimulated CBA increase, CBF increase, cell shrinkage, and $[Cl^-]_i$ decrease in airway ciliary cells (Figs. 1, 2, and 3). Figure 1 shows one ciliary beating cycle before (Fig. 1a) and 15 min after CCis stimulation (Fig. 1b). Figure 1 (a1–a9) shows consecutive images taken every 14–16 ms. A beating cilium was marked by a white line. Figure 1 (a1–a4) shows the effective stroke of the beating cilium, and Fig. 1 (a5–a9) shows the recovery stroke. The white line in Fig. 1 (a1) shows the start of effective stroke, Fig. 1 (a4) shows the end of effective stroke, and the line showing the start of effective stroke (Fig. 1 (a1)) is superimposed in Fig. 1 (a4). The angle between two lines in Fig. 1 (a4) shows the CBA [22]. Figure 1 (b1–b3) also shows the effective stroke of a beating cilium stimulated by CCis for 15 min, and Fig. 1 (b4–b7) shows the recovery stroke. The white line in Fig. 1 (b1) shows the start of effective stroke, Fig. 1 (b3) shows the end of effective stroke, and the line showing the start of effective stroke (Fig. 1 (b1)) is superimposed in Fig. 1 (b3). CCis stimulation increased the CBA from 94° (Fig. 1 (a4)) to 118° (Fig. 1 (b3)) and CBF from 9 Hz (Fig. 1 (a)) to 11 Hz (Fig. 1 (b)).

CCis stimulation also evoked cell shrinkage in airway ciliary cells. The outline of the airway ciliary cell before CCis stimulation is shown in Fig. 2a and is superimposed in Fig. 2b. As shown in Fig. 2 b, the ciliary cell 15 min after CCis stimulation was smaller than that just before CCis stimulation. Thus, CCis evoked cell shrinkage in airway ciliary cells. We measured $[Cl^-]_i$ of the airway ciliary cells using MQAE-based two-photon microscopy [19], because cell shrinkage under iso-osmotic conditions is known to decrease intracellular Cl^- concentration ($[Cl^-]_i$) [28, 29, 39]. Figure 2c, d shows changes in the MQAE fluorescence intensities of an airway ciliary cell just before and 15 min after CCis stimulation. CCis stimulation increased the intensity of MQAE fluorescence in an airway ciliary cell, indicating that CCis decreased $[Cl^-]_i$ as expected.

The enhancement of ciliary beating amplitude during CCis stimulation was detected by the light intensity change of a beating cilium reported by the image analysis program [50]. We selected the ciliary cells, beating cilia of which were observed from the apical side (Fig. 3 (a, b)). Figure 3 (a1, a2) shows the start and the end of effective stroke in an airway ciliary cell just before CCis stimulation. When we set a line "A-B" on video images of the beating cilium (Fig. 3 (a2)), the analysis program reported the image of light intensity changes on the line A-B (Fig. 3 (c)). The reported image shows the frequency and amplitude of ciliary beating [50]. Two white lines "S" and "E" in Fig. 3 (c) show the start and end of effective stroke, respectively. We measured the distance (pixels) between the two lines S and E, which is an index of ciliary beating amplitude (Fig. 3(c)). We expressed this amplitude as "CBA-D". Figure 3 (b1, b2) shows the start and the end of effective stroke in the same airway ciliary cell stimulated with CCis for 15 min. To analyze the ciliary beating 15 min after CCis stimulation, we set the line "C-D" on the same place of the cell. The analysis program reported changes in the light intensity on the line C-D. The reported image is shown in Fig. 3 (d). The amplitude of ciliary beating (CBA-D) 15 min after CCis stimulation (Fig. 3 (d)) was 25% larger than that just before CCis stimulation (Fig. 3 (c)). CCis stimulation also increased the frequency by 1 Hz (Figs. 3 (c, d)). Thus, Figs. 1 and 3 clearly showed that stimulation with CCis increased the amplitude (CBA and CBA-D) and the frequency (CBF) in the airway ciliary cells. In this study, we used CBA (angle) to evaluate the amplitude of airway ciliary beating.

Effects of CCis on CBF and CBA

The experiments were carried out in the presence of CO_2/HCO_3^-. Figure 4a shows a typical case. In an unstimulated airway ciliary cell, CBA and CBF were 100° and 11.5–12 Hz, respectively. Stimulation with 100 μM CCis gradually increased and plateaued CBA and CBF within 10–15 min, and CBA and CBF at the plateaus were 130° and 12–12.5 Hz, respectively. The concentration effects of CCis on CBA and CBF are shown in Fig. 4b, in which normalized CBA and CBF (CBA ratio and CBF ratio) are plotted. The stimulation with CCis (100 μM) gradually increased CBA and CBF, which reached plateaus within 15 min. The values of CBA ratio and CBF ratio 16 min after CCis stimulation were 1.25 ± 0.02 ($n = 6$) and 1.07 ± 0.02 ($n = 14$), respectively. In the CCis concentration-response study, CCis increased CBA and CBF in a concentration-dependent manner and maximally increased them at 100 μM (Fig. 4c). In the present study, the CCis concentration used for stimulation was 100 μM throughout the experiments. The experiments were also carried out in the absence of CO_2/HCO_3^- (Fig. 4d). The switch to CO_2/HCO_3^--free solution immediately increased CBA and CBF. The values of CBA ratio and CBF ratio 5 min after the switch were 1.16 ± 0.02 ($n = 5$) and 1.18 ± 0.03 ($n = 8$), respectively. Further CCis stimulation gradually increased CBA but not CBF. The values of CBA ratio and CBF ratio 16 min after CCis stimulation were 1.27 ± 0.02 ($n = 5$) and 1.18 ± 0.02 ($n = 8$), respectively. Thus, the CBA increase stimulated by CCis was independent of CO_2/HCO_3^-, while the CBF increase was dependent on CO_2/HCO_3^-. The CO_2/HCO_3^--free solution, which elevates pH_i [42, 44], increased CBA and CBF. Sutto et al. [42] showed that a pH_i elevation induced by the CO_2/HCO_3^--free solution increased CBF in tracheal

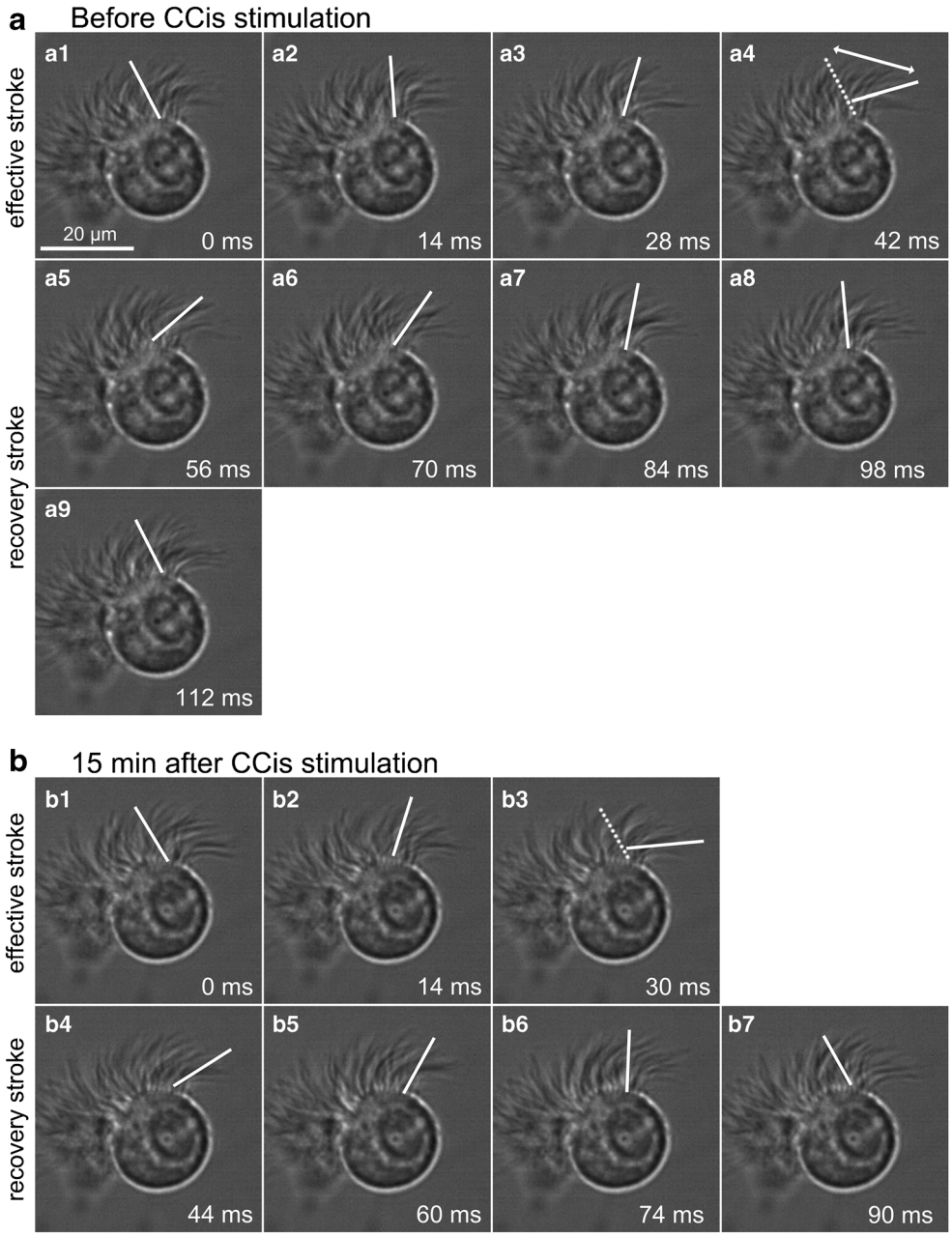

Fig. 1 Consecutive video images of an airway ciliary cell (side view). **a** Nine consecutive images taken every 14–16 ms showing one ciliary beating cycle before CCis stimulation. (a1–a4) show the effective stroke, and (a5–a9) show the recovery stroke. A beating cilium marked by white line in (a1) shows the start of effective stroke and that in (a4) shows the end of effective stroke, and the line showing the start of effective stroke (a1) is superimposed in (a4). The angle between two lines in (a4) shows the CBA [16]. **b** Seven consecutive images taken every 14–16 ms showing one ciliary beating cycle 15 min after CCis stimulation. (b1–b3) show the effective stroke, and (b4–b7) show the recovery stroke. A beating cilium marked by white line in (b1) shows the start of effective stroke and that in (b3) shows the end of effective stroke, and the line showing the start of effective stroke (b1) is superimposed in (b3). CCis stimulation increased the CBA from 94° (a4) to 118° (b3) and CBF from 9 Hz (**a**) to 11 Hz (**b**)

ciliary cells. This study also demonstrated that an elevation of pH_i induced by the CO_2/HCO_3^--free solution increases both CBA and CBF in the airway ciliary cells.

CCis stimulated cell shrinkage as shown in Fig. 2. Decreases in cell volume (V/V_0, an index of cell volume) are shown in Fig. 5a. The V/V_0 decreased and plateaued V/V_0 within 15 min from the start of CCis stimulation. The V/V_0 16 min after stimulation was 0.82 ± 0.02 ($n = 5$). Since the isosmotic cell shrinkage decreases $[Cl^-]_i$ [28], the $[Cl^-]_i$ was measured using MQAE-based two-photon microscopy (Fig. 5b) [19]. CCis stimulation decreased the ratio of MQAE fluorescence intensities (F_0/F) within 10 min. The value of F_0/F 10 min after stimulation was 0.78 ± 0.01 ($n = 4$). The time course of the decrease in $[Cl^-]_i$ was similar to that of the V/V_0 decrease (Fig. 5a, b). Changes in pH_i were also measured using carboxy-SNARF-1 during CCis stimulation (Fig. 5c). CCis stimulation slightly increased pH_i, although the increase in pH_i was not significant. The pH_is before and 20 min after CCis stimulation were 7.49 ± 0.02 and 7.54 ± 0.06, respectively ($n = 3$).

The effects of Ca^{2+}-free solution or a protein kinase A (PKA) inhibitor (PKI-A) on CCis-stimulated CBA and CBF were examined (Fig. 6a). We used a nominally Ca^{2+}-free solution to inhibit Ca^{2+} entry from the extracellular solution because EGTA-containing Ca^{2+}-free

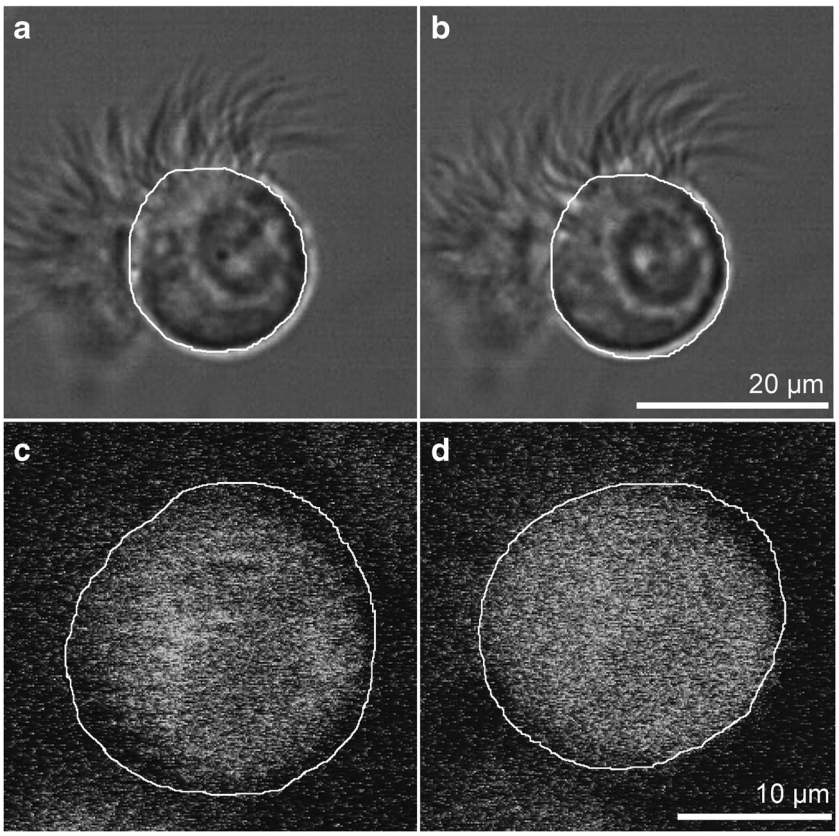

Fig. 2 Changes in cell volume and $[Cl^-]_i$ stimulated by CCis (100 μM). **a** A video image of an airway ciliary cell before CCis stimulation. The outline of a ciliary cell (white line) was depicted on a ciliary cell. **b** A video image of an airway ciliary cell 15 min after CCis stimulation. The white outline of the cell shows before CCis stimulation (**a**) and was superimposed on **b**. The outline of airway ciliary cell stimulated by CCis was smaller than that before CCis stimulation (white line). **c** The MQAE fluorescence image of an airway ciliary cell before CCis stimulation. **d** The MQAE fluorescence image of an airway ciliary cell 15 min after CCis stimulation. CCis potentiated the intensity of MQAE fluorescence, indicating that CCis stimulation decreased $[Cl^-]_i$

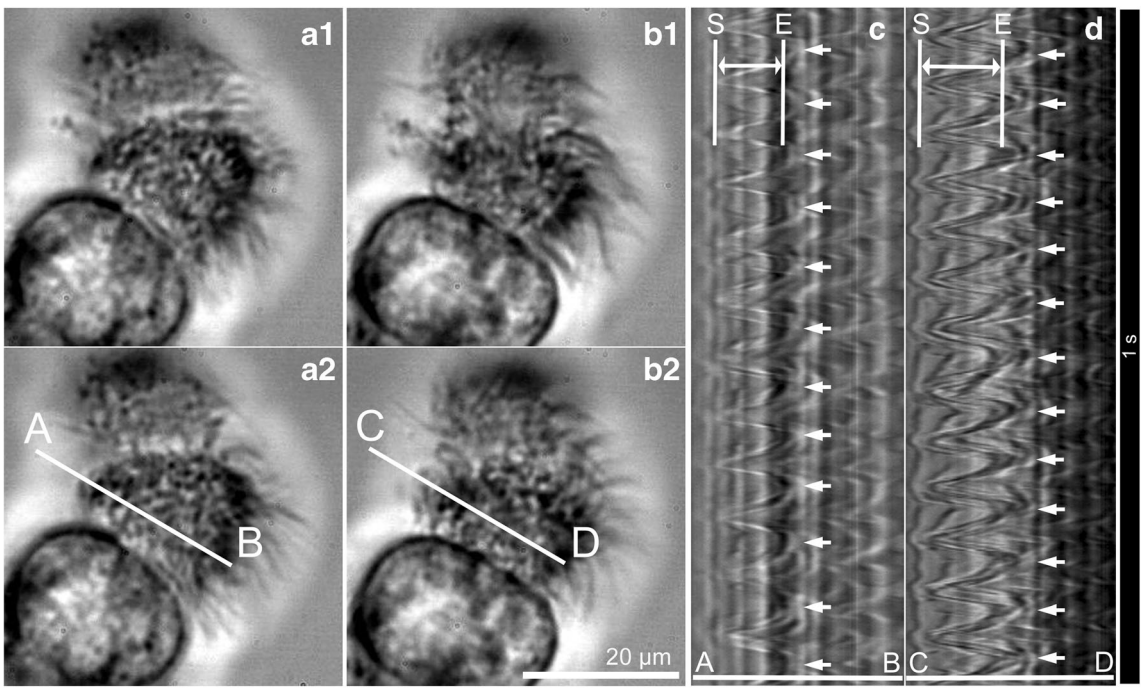

Fig. 3 Video images of airway ciliary cells (an apical view). We selected a visual field in which we could observe an airway ciliary cell from the vertical direction. **a** Before CCis stimulation. (a1) and (a2) show the start of and the end of a recovery stroke in a ciliary beating cycle, respectively. **b** Fifteen minutes after CCis stimulation. (b1) and (b2) show the start and the end of a recovery stroke, respectively. When we superimposed a line on the beating cilia (a line "A-B" on (a2) or "C-D" on (b2)), the analysis program reported the changes in light intensity of the line. **c** Changes in the light intensity of the line A-B in (a2) before CCis stimulation. **d** Changes in the light intensity of the line C-D in (b2) 15 min after CCis stimulation. Two white lines, "S" and "E" in (c) and (d) show the start and the end of an effective stroke. The reported image clearly shows that CCis increases the amplitude (distance between two lines S and E) and the frequency (marked by arrows, from 12 to 13 Hz) in the airway ciliary cells

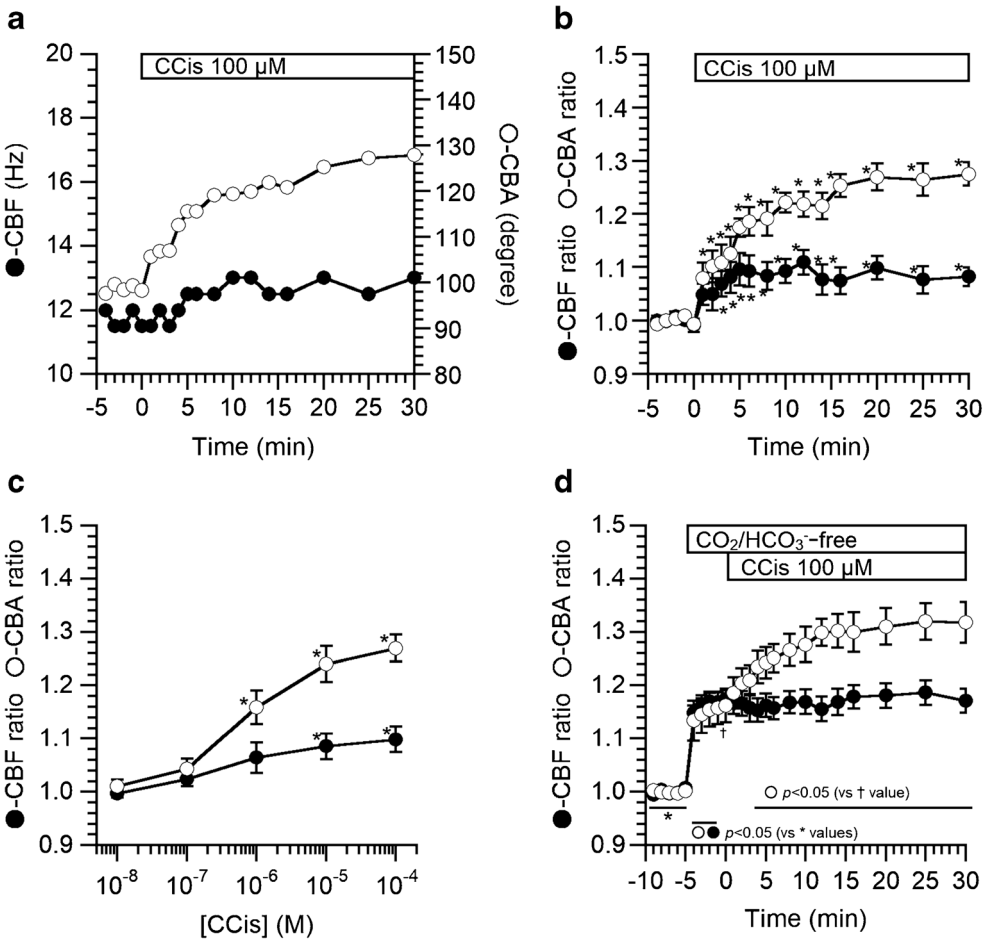

Fig. 4 Changes in CBA and CBF stimulated by CCis in airway ciliary cells. **a** A typical case. CCis (100 μM) stimulation increased CBA and CBF, which reached plateaus within 15 min. **b** Increases in normalized CBA (CBA ratio = CBA_t/CBA_0) and CBF (CBF ratio = CBF_t/CBF_0) during 100 μM CCis stimulation. Experiments were carried out in the presence of CO_2/HCO_3^-. CCis stimulation increased CBA by 30% and CBF by 10%. **c** The concentration-response study of CCis. CBA ratio and CBF ratio 15 min from the start of CCis stimulation were plotted. CCis at 100 μM maximally increased CBA and CBF in the airway ciliary cells. Significantly different (*$p < 0.05$). **d** The CCis-stimulated CBA and CBF increase in the absence of CO_2/HCO_3^-. The switch to the CO_2/HCO_3^--free solution immediately increased the CBA ratio (110%) and the CBF ratio (120%). Further CCis stimulation increased the CBA ratio to 130%, but not the CBF ratio

solution has been shown to stimulate cAMP accumulation by inhibiting PDE1A in airway ciliary cells [23, 24]. The switch to a nominally Ca^{2+}-free solution slightly decreased CBF by 5% but not CBA, as shown in the previous report [24]. The CBF ratio 5 min after the switch was 0.95 ± 0.01 ($n = 6$), while the CBA ratio 5 min after the switch was 1.02 ± 0.01 ($n = 5$). Further CCis stimulation increased CBA and CBF. The CBA ratio and CBF ratio 16 min after CCis stimulation were 1.18 ± 0.02 ($n = 5$) and 1.01 ± 0.03 ($n = 6$), respectively. Experiments were also carried out using airway ciliary cells treated with PKI-A for 30 min. Prior treatment with 1 μM PKI-A did not affect the increase in CBA or CBF stimulated by CCis (Fig. 6b). The CBA ratio and CBF ratio 16 min after CCis stimulation were 1.24 ± 0.01 ($n = 5$) and 1.05 ± 0.01 ($n = 5$), respectively. Thus, the CCis-induced increase in CBA and CBF was not mediated by an $[Ca^{2+}]_i$ increase nor a PKA activation.

pH_i pathway

CCis increased CBF dependent on CO_2/HCO_3^- as shown in Fig. 4. In the presence of CO_2/HCO_3^-, CCis slightly increased pH_i (Fig. 5). A previous study demonstrated that a pH_i elevation increases CBF [42]. These observations suggest that CCis increases CBF via a pH_i increase. The effects of DIDS (200 μM, a blocker of Na^+/HCO_3^- cotransport (NBC) and anion exchange (AE)) on CCis-stimulated CBA and CBF were examined (Fig. 7a). The addition of DIDS increased and sustained CBF but not CBA. The CBF ratio 10 min after DIDS addition was 1.06 ± 0.03 ($n = 22$), while the CBA ratio was 1.00 ± 0.01 ($n = 8$). Further CCis stimulation increased CBA but not CBF. The CBF ratio and CBA ratio 10 min after CCis stimulation were 1.15 ± 0.02 ($n = 22$) and 1.06 ± 0.02 ($n = 8$), respectively. On the other hand, DIDS is a well known inhibitor of volume-regulated anion channels and Ca^{2+}-activated Cl^- channels [4, 26, 27, 46]. Changes in cell volume induced by DIDS were measured to examine DIDS-sensitive Cl^- release from airway ciliary cells. If DIDS inhibited net Cl^- release in the airway ciliary cells, DIDS would increase cell volume. However, the addition of DIDS (200 μM) decreased V/V_0 to 0.92 ± 0.02 ($n = 5$) and the further addition of CCis decreased V/V_0 to 0.82 ± 0.02 ($n = 5$) (Fig. 7b). This indicates that DIDS does not inhibit net Cl^- efflux, suggesting that the Ca^{2+}-activated Cl^- channels are not main pathways for Cl^- release from airway ciliary cells. DIDS stimulated cell

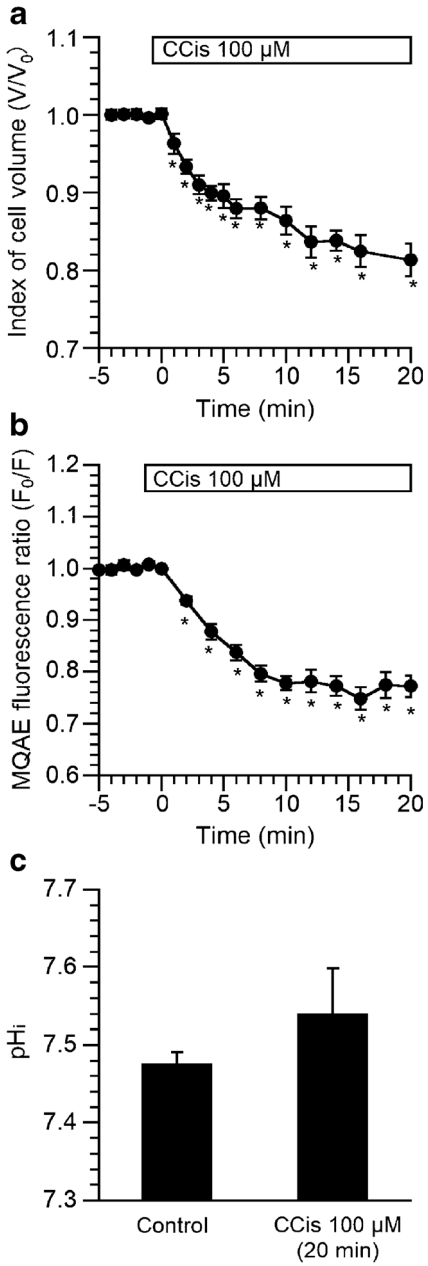

Fig. 5 Changes in cell volume, $[Cl^-]_i$ and pH_i stimulated by 100 μM CCis. **a** CCis-stimulated cell shrinkage. CCis stimulation gradually decreased cell volume to 80%. The cell volume reached a plateau 10 min from the start of CCis stimulation. **b** CCis-stimulated $[Cl^-]_i$ decrease. CCis decreased the MQAE fluorescence ratio (F_0/F) to 0.75. The time course of $[Cl^-]_i$ decrease was similar to that of cell shrinkage. Significantly different (*$p < 0.05$). **c** CCis-stimulated pH_i elevation. CCis stimulation slightly increased pH_i, but not significantly

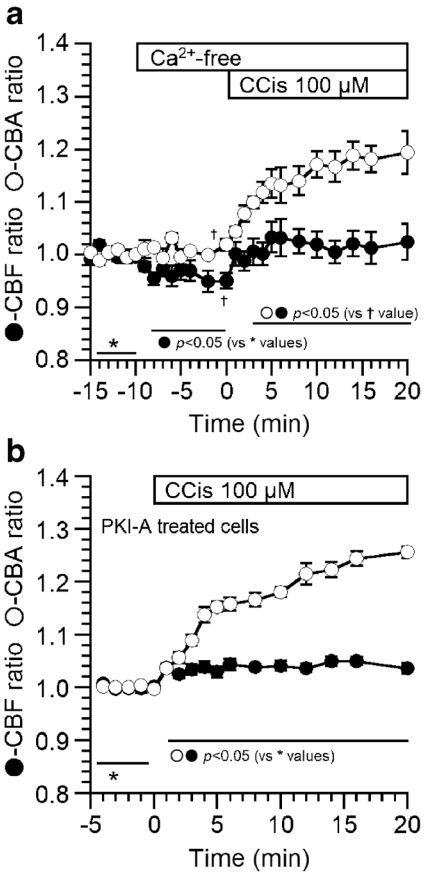

Fig. 6 The effects of Ca^{2+}-free solution and PKI-A (a PKA inhibitor) on CCis-stimulated CBA and CBF. **a** Ca^{2+}-free solution. The switch to a nominally Ca^{2+}-free solution decreased CBF to 0.95, but not CBA. Further CCis stimulation increased CBA by 30% and CBF by 10%. **b** PKI-A (1 μM). Cells were treated with PKI-A for 30 min prior to CCis stimulation. CCis stimulation increased CBA by 30% and CBF by 10%. Increases in CBA and CBF stimulated by CCis were not affected by the Ca^{2+}-free solution or PKI-A

shrinkage suggests that DIDS inhibits NBC and AE leading to inhibit NaCl entry, as shown in the following results. CCis still increased CBA without any CBF increase in the presence of DIDS, similar to the CO_2/HCO_3^--free solution. Changes in pH_i induced by DIDS were measured. The addition of DIDS gradually increased and plateaued pH_i within 10 min. The values of pH_i just before and 20 min after the DIDS addition were 7.44 ± 0.03 ($n = 5$) and 7.50 ± 0.03. Further CCis stimulation did not induce any increase in pH_i. To confirm NBC activation by CCis, experiments were carried out using HCO_3^--containing Cl^--free NO_3^- solution, in which NBC, not AE, functions (Fig. 7c). The switch to the HCO_3^--containing Cl^--free NO_3^- solution increased and sustained both CBA and CBF. The CBA ratio and CBF ratio 10 min after the switch were 1.13 ± 0.01 ($n = 8$) and 1.14 ± 0.02 ($n = 34$), respectively. Further CCis stimulation increased CBA and CBF. The CBA ratio and CBF ratio 20 min after CCis stimulation were 1.17 ± 0.02 ($n = 8$) and 1.22 ± 0.02 ($n = 34$), respectively (Fig. 7c). Changes in pH_i in the HCO_3^--containing Cl^--free NO_3^- solution were measured (Fig. 7d). The switch to the HCO_3^--containing Cl^--free NO_3^- solution increased pH_i. The values of pH_i just before and 10 min after the switch were 7.52 ± 0.01 ($n = 4$) and 7.63 ± 0.02, respectively. Further CCis stimulation increased pH_i. The value of pH_i 15 min after CCis stimulation was 7.71 ± 0.02 (Fig. 7d). Thus, in the HCO_3^--containing Cl^--free NO_3^- solution, CCis increased pH_i,

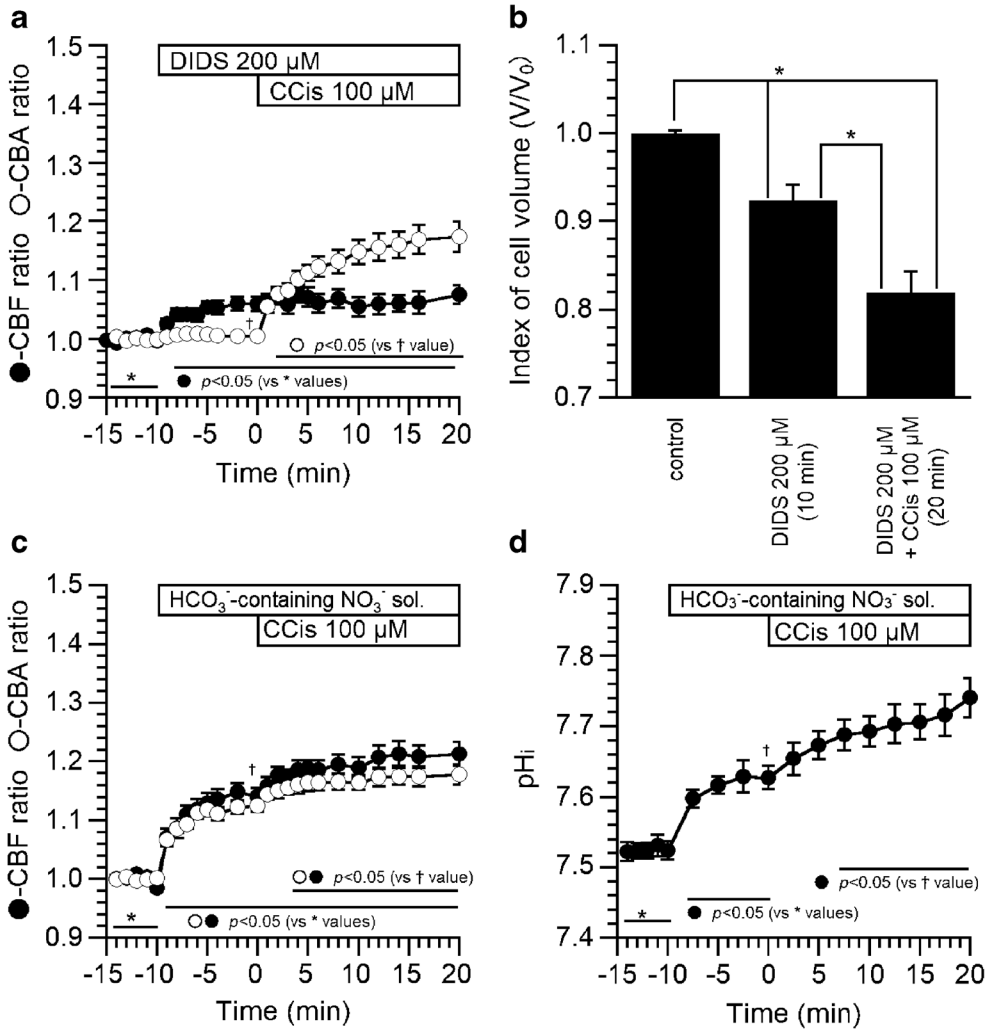

Fig. 7 The effects of DIDS and HCO_3^--containing Cl^--free solution (HCO_3^--containing NO_3^- solution) on CBA, CBF, and pH_i stimulated by CCis. **a** DIDS: The addition of DIDS gradually increased CBF, but not CBA. Further CCis stimulation increased the CBA ratio by 20%, but not the CBF ratio. **b** Changes in cell volume (V/V_0). The addition of DIDS (200 μM) decreased V/V_0 by 8%, suggesting DIDS inhibit NaCl entry via NBC and AE, but not net Cl^- release. Further CCis stimulation decreased V/V_0, suggesting that CCis stimulated Cl^- release are not inhibited by DIDS. **c** HCO_3^--containing NO_3^- solution, in which NBC functions, but not AE. This solution also decreases $[Cl^-]_i$ to an extremely low level by replacing Cl^- with NO_3^-. The switch to HCO_3^--containing NO_3^- solution immediately increased both CBA and CBF, and further CCis stimulation increased CBA and CBF. **d** Changes in pH_i in the HCO_3^--containing NO_3^- solution. The switch to HCO_3^--containing NO_3^- solution immediately increased pH_i. Further CCis stimulation increased pH_i, suggesting that CCis stimulates NBC to increase HCO_3^- entry

indicating that CCis stimulates NBC leading to a pH_i increase (HCO_3^- entry). These observations suggest that a small pH_i increase (activation of the pH_i pathway) stimulated by CCis increases CBA and CBF in the control solution, although the extent of CBA increase may be small.

Cl^- pathway

In airway ciliary cells, cell shrinkage has been shown to modulate CBF increase during terbutaline stimulation [38]. The isosmotic cell shrinkage has been shown to decrease $[Cl^-]_i$ [28], and moreover, an $[Cl^-]_i$ decrease has been shown to modulate some cellular functions [15, 17, 28, 29, 39, 40, 43]. The effects of an $[Cl^-]_i$ decrease stimulated by CCis on CBA and CBF were examined. To examine whether CCis inhibits NKCC to decrease $[Cl^-]_i$, we used bumetanide (20 μM, an inhibitor of $Na^+/K^+/2Cl^-$ cotransport (NKCC)) (Fig. 8a). The addition of bumetanide alone increased CBA but not CBF. The CBA ratio and CBF ratio 10 min after bumetanide addition were 1.11 ± 0.01 ($n = 4$) and 1.00 ± 0.01 ($n = 9$), respectively. Further CCis stimulation increased both CBA and CBF. The CBA ratio and CBF ratio 10 min after CCis stimulation were 1.25 ± 0.01 ($n = 4$) and 1.07 ± 0.02 ($n = 9$), respectively. We also measured $[Cl^-]_i$ in MQAE-loaded airway ciliary cells using the same protocol. Figure 8b shows changes in F_0/Fs in three experiments. The

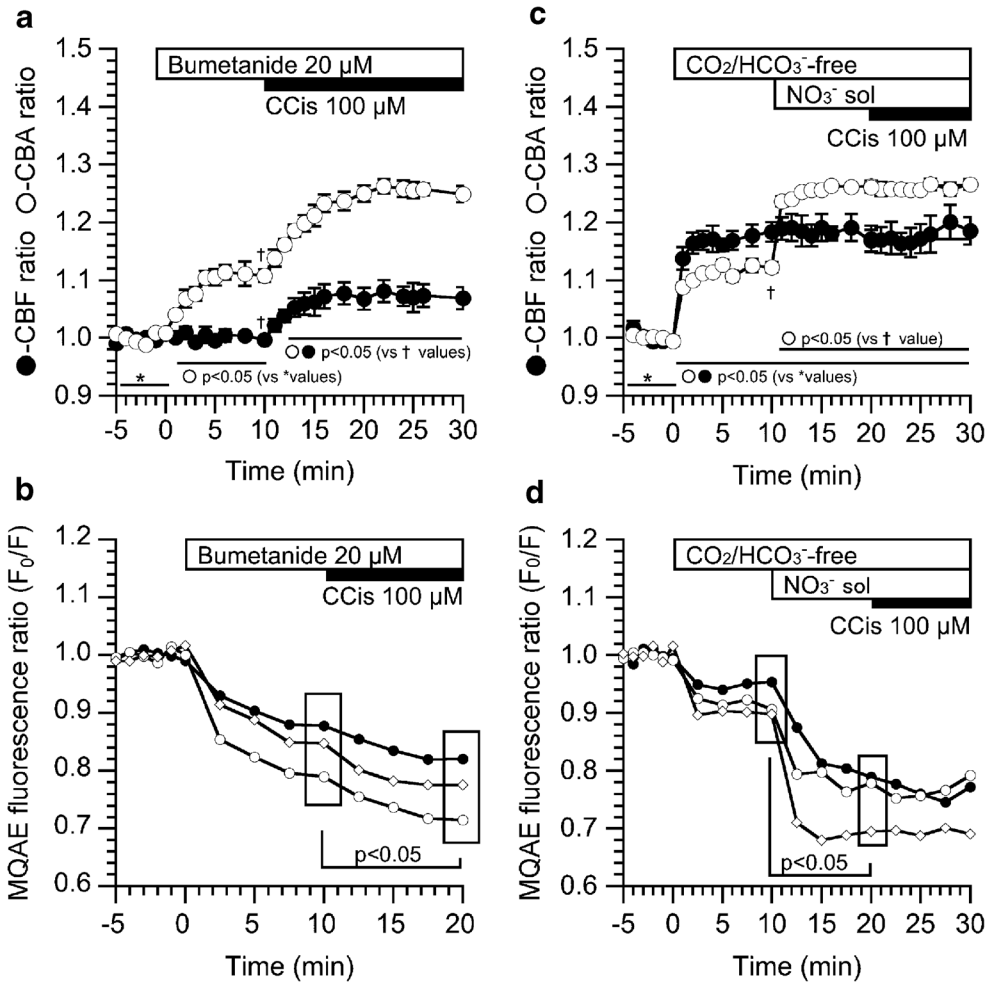

Fig. 8 The effects of bumetanide and Cl^--free solution (NO_3^- solution) on CCis-stimulated CBA and CBF. **a** CBA and CBF increases stimulated by CCis in the presence of bumetanide (an NKCC inhibitor) under the CO_2/HCO_3^--containing condition. The addition of bumetanide increased CBA, but not CBF. Further CCis stimulation increased CBA and CBF. **b** Changes in $[Cl^-]_i$ induced by CCis in the presence of bumetanide. Changes in F_0/F were obtained from three experiments. The addition of bumetanide decreased F_0/F, and further stimulation with CCis decreased F_0/F. CCis significantly decreased F_0/F ($p < 0.05$, paired t test). **c** CBA and CBF increases stimulated by CCis in the CO_2/HCO_3^--free Cl^--free NO_3^- solution. The switch to NO_3^- solution immediately increased CBA, but not CBF. Further CCis stimulation did not induce any increase in CBA or CBF. **d** Changes in $[Cl^-]_i$ induced by CCis in the CO_2/HCO_3^--free Cl^--free NO_3^- solution. The switch to the CO_2/HCO_3^--free solution alone decreased $[Cl^-]_i$. The second switch to NO_3^- solution further decreased $[Cl^-]_i$, and further CCis stimulation did not change $[Cl^-]_i$

addition of bumetanide (20 μM) alone decreased and plateaued F_0/F within 3 min. The value of F_0/F 10 min after bumetanide addition was 0.83 ± 0.03 ($n = 3$). Then, further addition of CCis decreased F_0/F (F_0/F 10 min after CCis stimulation $= 0.77 \pm 0.03$, $n = 3$). Thus, in the presence of bumetanide, CCis still decrease $[Cl^-]_i$, indicating that CCis does not inhibit NKCC (the $[Cl^-]_i$ decrease stimulated by CCis was not caused by inhibition of NKCC). However, the addition of bumetanide alone, which decreased $[Cl^-]_i$, increased CBA (Fig. 8a), suggesting that a decrease in $[Cl^-]_i$ increased CBA, but not CBF.

To decrease $[Cl^-]_i$, experiments were carried out using CO_2/HCO_3^--free Cl^--free NO_3^- solution (Fig. 8c). The CO_2/HCO_3^--free Cl^--free NO_3^- solution has already been shown to decrease $[Cl^-]_i$ by substituting NO_3^- for Cl^- in airway ciliary cells [19]. The switch to CO_2/HCO_3^--free solution increased CBA and CBF (CBA ratio and CBF ratio 10 min after the switch were 1.12 ± 0.01 ($n = 4$) and 1.18 ± 0.02 ($n = 5$), respectively). Then, the second switch to CO_2/HCO_3^--free Cl^--free NO_3^- solution immediately increased CBA but not CBF. The values of CBA ratio and CBF ratio 10 min after the switch were 1.26 ± 0.01 and 1.17 ± 0.02, respectively. Further CCis stimulation did not induce any increase in CBA or CBF (Fig. 8c). $[Cl^-]_i$ was also measured using the same protocol, and Fig. 8d shows changes in F_0/Fs in three experiments. The switch to CO_2/HCO_3^--free solution decreased $[Cl^-]_i$ (F_0/F 10 min after the switch $= 0.92 \pm 0.01$, $n = 4$). Then, the second switch to the CO_2/HCO_3^--free Cl^--free NO_3^- solution further decreased $[Cl^-]_i$ (F_0/F 10 min after the second switch $= 0.75 \pm 0.03$), and then CCis stimulation did not induce any change in $[Cl^-]_i$.

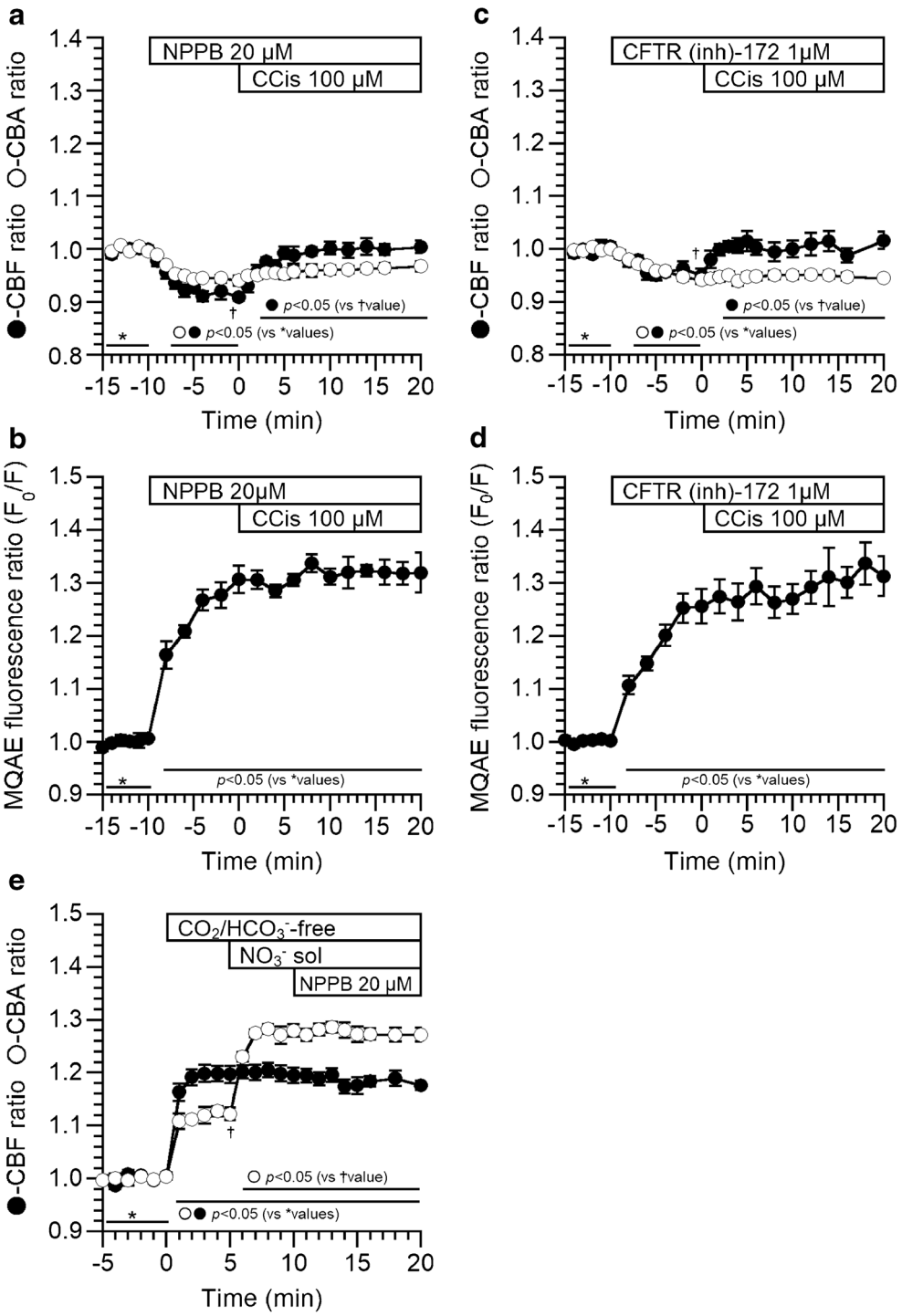

Fig. 9 Effects of the Cl^- channel blockers (NPPB and CFTR(inh)-172) on CBA, CBF, and $[Cl-]_i$ stimulated by CCis. **a**, **b** NPPB (20 μM). **a** Changes in CBA and CBF. The addition of NPPB alone decreased CBA and CBF by 8–10%. Further CCis stimulation increased CBF by 10% and slightly increased CBA. **b** Changes in MQAE fluorescence ratio (F_0/F). NPPB increased $[Cl^-]_i$, and further CCis stimulation did not induce any change in F_0/F. **c**, **d** CFTR(inh)-172 (1 μM). **c** Changes in CBA and CBF. The addition of CFTR(inh)-172 alone decreased CBA and CBF by 4–5%. Further CCis stimulation increased CBF by 5% and not CBA. **d** Changes in MQAE fluorescence ratio (F_0/F). CFTR(inh)-172 increased $[Cl^-]_i$, and further CCis stimulation did not induce any change in F_0/F. Increases in F_0/F induced by CFTR(inh)172 were slightly small compared with those induced by NPPB. **e** Effects of NPPB on CBF, and CBA. The CO_2/HCO_3^--free Cl^--free NO_3^- solution does not induce any change in pH_i affected by CO_2/HCO_3^- and in $[Cl^-]_i$. In the CO_2/HCO_3^--free Cl^--free NO_3^- solution, addition of NPPB did not induce any change in CBF or CBA, suggesting that 20 μM NPPB-induced pH_i decrease was negligibly small

To counteract the increase in $[Cl^-]_i$, the airway ciliary cells were treated with a Cl^- channel blocker (20 μM NPPB) (Fig. 9a, b). The addition of NPPB induced a small decrease in CBA and CBF. The CBA ratio and CBF ratio 10 min after NPPB addition were 0.95 ± 0.01 ($n = 5$) and 0.91 ± 0.01 ($n = 12$), respectively. Further, CCis stimulation increased CBF but not CBA. The CBA ratio and CBF ratio 10 min after CCis stimulation were 0.96 ± 0.01 ($n = 5$) and 1.00 ± 0.01 ($n = 12$), respectively (Fig. 9a). This suggests that CCis appears to increase pH_i in the presence of NPPB leading to a CBF increase. We also measured $[Cl^-]_i$ using MQAE fluorescence. The addition of NPPB increased $[Cl^-]_i$ (F_0/F 10 min after the NPPB addition = 1.31 ± 0.03, $n = 4$), but further CCis stimulation did not induce any change in $[Cl^-]_i$ (F_0/F 10 min after the NPPB addition = 1.31 ± 0.03, $n = 4$) (Fig. 9b).

Experiments were also carried out using CFTR(inh)-172 (1 μM, an inhibitor of CFTR) (Fig. 9c, d). Because, previous studies [12, 25, 30] suggest that CCis stimulates CFTR in human airways. CFTR(inh)-172 evoked similar responses in CBA, CBF, and $[Cl^-]_i$, although extents of decreases in CBA and CBF or in $[Cl^-]_i$ increase were slightly small. The CBA ratio and CBF ratio 10 min after CFTR(inh)-172 addition were 0.94 ± 0.01 ($n = 6$) and 0.95 ± 0.01 ($n = 10$), respectively. Further CCis stimulation increased CBF (1.02 ± 0.02, $n = 10$) not CBA (0.95 ± 0.01, $n = 5$) (Fig. 9c). Changes in $[Cl^-]_i$ were measured using MQAE fluorescence. The addition of CFTR(inh)-172 increased $[Cl^-]_i$. The value of F_0/F 10 min after CFTR(inh)-172 addition was 1.26 ± 0.03 ($n = 4$). Then, further CCis stimulation did not induce any change in $[Cl^-]_i$ (F_0/F 10 min after CFTR(inh)-172 addition = 1.27 ± 0.03, $n = 4$) (Fig. 9d). Thus, CCis appears to stimulate CFTR in mouse airways, as shown in human airways [12, 30].

On the other hand, NPPB has been reported to decrease pH_i at high concentration, such as 100 μM [8]. A decrease in pH_i has been reported to reduce CBF [42]. To examine the effects of NPPB on pH_i, CBF and CBA were measured in the CO_2/HCO_3^--free Cl^--free NO_3^- solution, which did not induce any change in pH_i affected by CO_2/HCO_3^- and in $[Cl^-]_i$. In the CO_2/HCO_3^--free Cl^--free NO_3^- solution, addition of NPPB did not induce any change in CBF or CBA (Fig.9e). This suggests that, at 20 μM NPPB, a decrease in pH_i was negligibly small.

Thus, NPPB or CFTR(inh)-172 abolished the CBA increase, CBF increase, and $[Cl^-]_i$ decrease stimulated by CCis, indicating that CCis activates Cl^- channels, as previously reported [10, 25, 30]. Thus, an increase in $[Cl^-]_i$ decreases CBF and CBA, but a decrease in $[Cl^-]_i$ increases only CBA.

CFTR expression

This study shows that CCis stimulates Cl^- release from ciliary cells via Cl^- channels including CFTR. The previous studies demonstrated that CFTR does not express in ciliary cells of rodent trachea and bronchi [14, 15]. The Western blot analysis for CFTR was carried out using isolated lung cells and striated muscles of thigh. In the isolated lung cells, the band for CFTR (168 kDa) was detected, but not in the striated muscles (Fig. 10a). The localization of CFTR of airway ciliary cells was examined using confocal immunofluorescence microscopy (Fig. 10b). Figure 10 (A) shows an airway ciliary cell. Airway ciliary cells were immunopositively stained for CFTR, which localizes in the cilia and the cytoplasm. The immunofluorescence of ARL13B (a small ciliary G protein localized in cilia) was positive in the cilia located in the apical surface (Fig. 10 (B)). Merged image shows CFTR exists in the airway cilia and cell body (Fig. 10 (C)). Figure 10 (D) shows the phase contrast image of an airway ciliary cell.

Discussion

This study demonstrated that CCis increases CBA by 30% and CBF by 10% in the airway ciliary cells of mice, mediated via a pH_i elevation (pH_i pathway) and an $[Cl^-]_i$ decrease (Cl^- pathway). The pH_i pathway, which is CO_2/HCO_3^--dependent, increases both CBA and CBF by 5–10%, and the Cl^- pathway, which is CO_2/HCO_3^--independent, only increases CBA by 20%.

The Cl^- pathway is the main pathway to increase CBA during CCis stimulation. CCis stimulation activates Cl^- channels, leading to a decrease in $[Cl^-]_i$. A decrease in $[Cl^-]_i$ increases CBA, and an increase in $[Cl^-]_i$ decreases both CBA and CBF. At present, the mechanisms by which intracellular Cl^- may regulate IDAs and ODAs are still unknown. A previous study showed that microtubule activation of the brain cytoplasmic dynein (ATPase activity) is stimulated by a low concentration of KCl, suggesting that a decrease in $[Cl^-]_i$ increases the affinity of the dynein for microtubules [41]. Similar mechanisms may regulate the activity of IDA- or ODA-ATPase in the airway cilia. However, the effects of $[Cl^-]_i$ on CBA are different from those on CBF, that is, a decrease in $[Cl^-]_i$ increased only CBA but not CBF, and in contrast, an increase in $[Cl^-]_i$ decreased both CBF and CBA. One possible explanation is that the dependency on $[Cl^-]_i$ of CBA may be different from that of CBF in airway cilia, such that the $[Cl^-]_i$-response curve of CBA shifts to a lower concentration than that of CBF.

There are many reports showing that a decrease in $[Cl^-]_i$ enhances some cellular functions [15, 17, 28, 29, 31, 38–40, 43, 45], including CBF increase in airway ciliary cells [38, 45]. The present study also showed that changes in $[Cl^-]_i$ appear to modulate CBA and CBF in airway ciliary cells.

The present study demonstrated that CCis activates Cl^- channels to increase Cl^- release in airway ciliary cells.

There are evidences showing that CCis increases Cl^- secretion in airway epithelial cells [10, 25], although the mechanisms are not fully understood [16]. CCis is known to have a variety of effects on the mucociliary clearance [16, 18, 36]. The present study suggests that CCis stimulation activates airway mucociliary clearance by enhancing ciliary beating and Cl^- secretion.

Airway epithelial cells including ciliary cells have many types of Cl^- channels, such as CFTR and Ca^{2+}-activated Cl^- channels [13, 14]. In previous studies, CCis stimulated the activity and the density of active cAMP-dependent channels, identical to the CFTR channel, in human respiratory epithelium [12, 30]. The present study

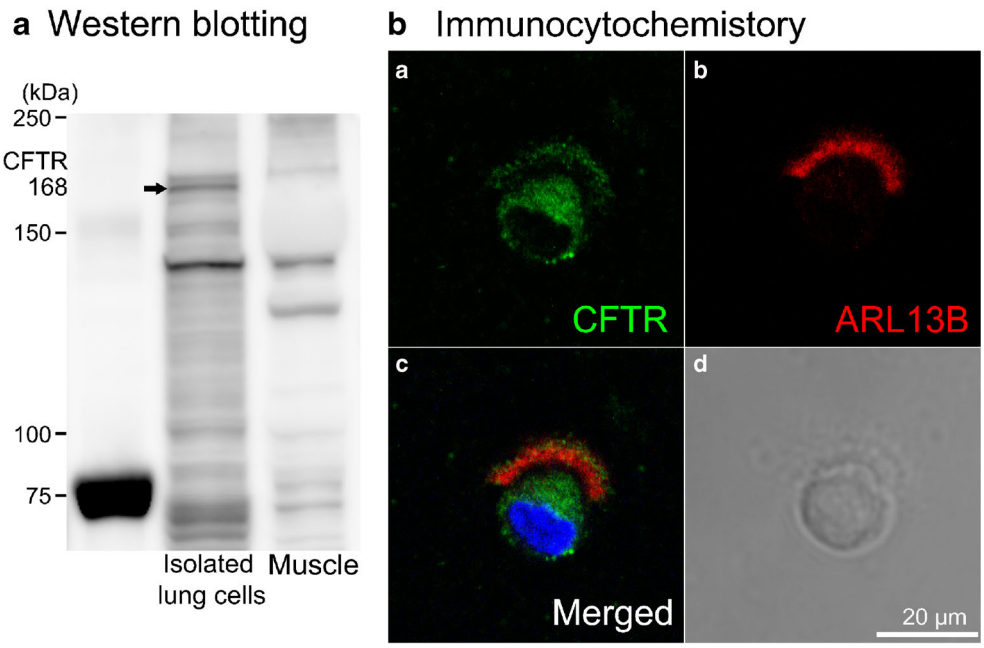

Fig. 10 Expression of CFTR in airway ciliary cells. **a** Western blotting. In the isolated lung cells including airway ciliary cells (~ 20%), the band for CFTR (168 kDa) were detected, but not in the striated muscles. **b** Immunofluorescence examination. (a) CFTR. Airway ciliary cells were immunopositively stained for CFTR, which localizes in the cilia and the cell body. (b) ARL13B (a small ciliary G protein localized in cilia). The immunofluorescence of ARL13B was positive in the cilia located in the apical surface. (c) Marged. The merged image shows that CFTR exists in the cilia and cell body in the airway ciliary cells. (d) Phase contrast image

also showed that CFTR expresses in mouse lung airway ciliary cells and plays a crucial role for decreasing $[Cl^-]_i$. However, previous studies showed that CFTR does not exist in ciliated cells in the trachea or bronchus of the rodent [13, 14]. In our experiments, the airway ciliary cells used were isolated from lung, not from trachea and bronchi. The differences in the CFTR expression between the previous studies [13, 14] and the present study may be explained by those between proximal and distal airways. There are reports showing that CBF regulation in distal airways is different from that in trachea [11].

On the other hand, DIDS inhibits Ca^{2+}-activated Cl^- channels [4, 26, 27, 46], although we used it as an inhibitor of NBC and AE. Since the addition of DIDS increases pH_i and decreases cell volume, it is certain that DIDS inhibits NBC and AE. The DIDS-induced decrease in cell volume indicates that DIDS did not inhibit the net Cl^- release. If DIDS-sensitive Cl^- channels are the main pathways for Cl^- release, DIDS should increase cell volume. However, DIDS decreased cell volume in airway ciliary cells. These results suggest that the DIDS-sensitive Cl^- channels are not main pathways for Cl^- release from airway ciliary cells. Moreover, CCis decreased cell volume in the presence of DIDS. Thus, a decrease in $[Cl^-]_i$ stimulated by CCis is induced by activation of the Cl^- channels other than DIDS-sensitive Ca^{2+}-activated Cl^- channels, such as CFTR Cl^- channels in airway ciliary cells.

On the other hand, CBF increases stimulated by CCis were dependent on CO_2/HCO_3^-, suggesting a pH_i elevation induced by HCO_3^- entry increase CBF [42, 44]. However, the extent of pH_i increase stimulated by CCis was small (not

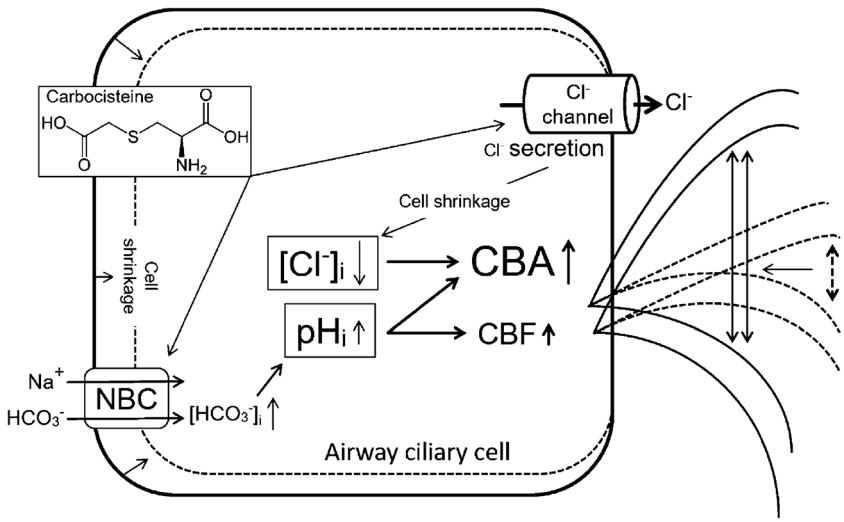

Fig. 11 CCis stimulated CBA and CBF increase in the airway ciliary cell. CCis activated the pH_i pathway and the Cl^- pathway to increase CBA and CBF

significant). We examined the effects of CCis on pH_i in the CO_2/HCO_3^--containing Cl^--free NO_3^- solution in which NBC functions. In this solution, CCis significantly increased pH_i, indicating that CCis stimulates NBC leading to enhance HCO_3^- entry. We believe that CCis stimulates a small pH_i elevation in airway ciliary cells, and this small pH_i elevation stimulated by CCis increases CBF. However, it is unclear whether a small elevation of pH_i stimulated by CCis increases CBA. The extent of CBA increase stimulated by CCis in the CO_2/HCO_3^--free solution was smaller than that in the CO_2/HCO_3^--containing solution. This suggests that activation of the pH_i pathway by CCis increases CBA, although the extent of the CBA increase would be small (approximately by 5–10%). Inhibition of AE also increases pH_i through inhibition of HCO_3^- exit from cells. However, at present, we do not know whether or not CCis inhibits AE. Further experiments are required to clarify the effects of CCis on AE.

A pH_i increase has already been shown to increase CBF in human airway cilia and sperm flagella [20, 32, 42]. A pH_i increase is suggested to act directly on ODAs in sperm flagella to increase CBF [20]. Although there is no report showing that an elevation of pH_i stimulates IDAs, a pH_i increase may also stimulate IDAs leading to CBA increase, similarly to ODAs. There are reports showing that the pH_i affects dyneins; pH_i-induced changes in the histidine charge affect dynein ATPase activity [3], and a pH_i increase stimulates the pH-dependent and cAMP-independent phosphorylation of dynein components and/or other axonemal proteins [32]. Although the exact mechanisms for pH_i regulation of ODAs or IDAs are unknown, these mechanisms activated by a pH_i increase may stimulate IDA and ODA.

A previous study showed that CCis did not increase CBF in tracheal ciliary cells [33]. However, their experiments were performed at room temperature (25–26 °C). Because CBF responses are well known to be temperature-dependent [11], the room temperature appears to mask the CBF increase stimulated by CCis because of a small CBF increase.

The conclusions of this study are summarized in Fig. 11. CCis activates the pH_i pathway and the Cl^- pathway. In the pH_i pathway, CCis activates HCO_3^- entry via NBC, which elevates the pH_i of the airway ciliary cells. This pH_i elevation increases both CBF and CBA by 10%. In the Cl^- pathway, CCis activates Cl^- channels, including CFTR. The activation of Cl^- channels stimulates Cl^- release from cells, leading to $[Cl^-]_i$ decrease. The $[Cl^-]_i$ decrease increases CBA by 20%. CCis may activate the activity and increase the number of Cl^- channels, as shown in previous reports obtained from human airways [12, 30].

Acknowledgements We thank Osaka Medical College for giving us an opportunity to perform the experiments using the video microscope equipped with a high-speed camera.

Funding This work was partly supported by Grants-in-Aid for Scientific Research from the Japan Society of the Promotion of Science to YM (No. JP18H03182) and to SH (No. 17K08545).

Compliance with ethical standards

The procedures and protocols for the experiments were approved by the Committee for Animal Research of Kyoto Prefectural University of Medicine (No. 26-263) and Ritsumeikan University (No. BKC 2017-050). The animals were cared for, and the experiments were carried out according to the guidelines of this committee. Female mice (C57BL/6J, 6 weeks of age) were purchased from Shimizu Experimental Animals (Kyoto, Japan) and fed standard pellet food and water ad libitum.

Conflict of interest The authors declare that they have no conflict of interest.

References

1. Afzelius BA (2004) Cilia-related diseases. J Pathol 204:470–477
2. Arora K, Huang Y, Mun K, Yariagadda S, Sundram N, Kessler MM, Hannig G, Kurtz CB, Silos-Santiago I, Helmrath M, Palermo JJ, Clancy JP, Steinbrecher KA, Naren AP (2017) Guanylate cyclase 2C agonism corrects CFTR mutants. JCI Insight 2(19):e93686. https://doi.org/10.1172/jci.insight.93686
3. Barbar E, Kleinman B, Imhoff D, Li M, Hays TS, Hare M (2001) Dimerization and folding of LC8, a highly conserved light chain of cytoplasmic dynein. Biochemistry 40:1596–1605
4. Benedetto R, Ousingswat J, Wanitchakool P, Zhang Y, Holtzman MJ, Amaral M, Rock JR, Schreiber R, Kunzelmann K (2017) Epithelial chloride transport by CFTR requires TMEM16A. Sci Rep 7:12397. https://doi.org/10.1038/s41598-017-10910-0
5. Bridges RJ (2012) Mechanisms of bicarbonate secretion: lessons from the airways. Cold Spring Harb Prespect Med 2:a015016
6. Brokaw CJ, Kamiya R (1987) Bending patterns of *Chlamydomonas* flagella: IV. Mutants with defects in inner and outer dynein arms indicate differences in dynein arm function. Cell Motil Cytoskeleton 8:68–75
7. Brokaw CJ (1994) Control of flagellar bending: a new agenda based on dynein diversity. Cell Motil Cytoskeleton 28:199–204
8. Brown CDA, Dudley AJ (1996) Chloride channel blockers decrease intracellular pH in cultured renal epithelial LLC-PK1 cells. Br J Pharmacol 118:443–444
9. Chen WY, Xu WM, Chen ZH, Ni Y, Yuan YY, Zhou SC, Zhou WW, Tsang LL, Chung YW, Höglund P, Chan HC, Shi QX (2009) Cl^- is required for HCO_3^- entry necessary for sperm capacitation in guinea pig: involvement of a Cl^-/HCO_3^- exchanger (SLC26A3) and CFTR. Biol Reprod 80:115–123
10. Colombo B, Turconi P, Daffonchio L, Fedele G, Omini C, Cremaschi D (1994) Stimulation of Cl^- secretion by the mucoactive drug S-carboxymethylcysteine-lysine salt in the isolated rabbit trachea. Eur Respir J 7:1622–1628
11. Delmotte P, Sanderson MJ (2006) Ciliary beat frequency is maintained at a maximal rate in the small airways of mouse lung slices. Am J Respir Cell Mol Biol 35:110–117
12. Guizzardi F, Rodighiero S, Binelli A, Saino S, Bononi E, Dossena S, Garavaglia ML, Bazzini C, Bottà G, Conese M, Daffonchio L, Novellini R, Paulmichl M, Meyer G (2006) S-CMC-Lys-dependent stimulation of electrogenic glutathione secretion by human respiratory epithelium. J Mol Med 84:97–107
13. Hahn A, Faulhaber J, Srisawang L, Stortz A, Salomon JJ, Mall MA, Frings S, Möhrlen F (2017) Cellular distribution and function of ion channels involved in transport processes in rat tracheal epithelium.

Physiol Rep 5(12):e13290. doi: https://doi.org/10.14814/phy2.13290
14. Hahn A, Salomon JJ, Leitz D, Feigenbutz D, Korsch L, Lisewski I, Schrimpf K, Millar-Büchner P, Mall MA, Frings S, Möhrlen F (2018) Expression and function of Anoctamin 1/TMEM16A calcium-activated chloride channels in airways of in vivo mouse models for cystic fibrosis research. Pflügers Arch 470:1335–1348. https://doi.org/10.1007/s00424-018-2160-x
15. Higashijima T, Ferguson KM, Sternweis PC (1987) Regulation of hormone-sensitive GTP-dependent regulatory proteins by chloride. J Biol Chem 262:3597–3602
16. Hooper C, Calvert J (2008) The role for S-carboxymethylcysteine (carbocisteine) in the management of chronic obstructive pulmonary disease. Int J COPD 3:659–669
17. Hosogi S, Kusuzaki K, Inui T, Wang X, Marunaka Y (2014) Cytosolic chloride ion is a key factor in lysosomal acidification and function of autophagy in human gastric cancer cell. J Cell Mol Med 18:1124–1133
18. Houtmeyers E, Gosselink R, Gayan-Ramirez G, Decramer M (1999) Effects of drugs on mucus clearance. Eur Respir J 14:452–467
19. Ikeuchi Y, Kogiso H, Hosogi S, Tanaka S, Shimamoto C, Inui T, Nakahari T, Marunaka Y (2018) Measurement of $[Cl^-]_i$ unaffected by the cell volume change using MQAE-based two-photon microscopy in airway ciliary cells of mice. J Physiol Sci 68:191–199
20. Keskes L, Giroux-Widemann V, Serres C, Pignot-Paintrand I, Jouannet P, Feneux D (1998) The reactivation of demembranated human spermatozoa lacking outer dynein arms is independent of pH. Mol Reprod Dev 49:416–425
21. Kim D, Kim J, Burghardt B, Best L, Steward MC (2014) Role of anion exchangers in Cl^- and HCO_3^- secretion by the human airway epithelial cell line Calu-3. Am J Physiol Cell Physiol 307:C208–C219
22. Komatani-Tamiya N, Daikoku E, Takemura Y, Shimamoto C, Nakano T, Iwasaki Y, Kohda Y, Matsumura H, Marunaka Y, Nakahari T (2012) Procaterol-stimulated increases in ciliary bend amplitude and ciliary beat frequency in mouse bronchioles. Cell Physiol Biochem 29:511–522
23. Kogiso H, Hosogi S, Ikeuchi Y, Tanaka S, Shimamoto C, Matsumura H, Nakano T, Sano K, Inui T, Marunaka Y, Nakahari T (2017) A low $[Ca^{2+}]_i$-induced enhancement of cAMP-activated ciliary beating by PDE1A inhibition in mouse airway cilia. Pflügers Arch Eur J Physiol 469:1215–1227
24. Kogiso H, Hosogi S, Ikeuchi Y, Tanaka S, Inui T, Marunaka Y, Nakahari T (2018) $[Ca^{2+}]_i$ modulation of cAMP-stimulated ciliary beat frequency via PDE1 in airway ciliary cells of mice. Exp Physiol 103:381–390
25. Köttgen M, Busch AE, Hug MJ, Greger R, Kunzelman K (1996) N-acetyl-L-cysteine and its derivatives activate a Cl^- conductance in epithelial cells. Pflügers Arch Eur J Physiol 431:549–555
26. Kurita T, Yamamura H, Suzuki Y, Giles WR, Imaizumi Y (2015) The CLC-7 chloride channel is downregulated by hypoosmotic stress in human chondrocytes. Mol Pharmacol 88:113–120
27. Liu Y, Zhang H, Qi J, Xu J, Gao H, Du X, Gamper N, Zhang H (2015) Characterization of effects of Cl^- channel modulators on TMEM16A and bestrophin-1 Ca^{2+} activated Cl^- channels. Pflügers Arch 467:1417–1430
28. Marunaka Y (1997) Hormonal and osmotic regulation of NaCl transport in renal distal nephron epithelium. Jpn J Physiol 47:499–511
29. Marunaka Y (2017) Actions of quercetin, a flavonoid, on ion transporters: its physiological roles. Ann N Y Acad Sci 1398:142–151
30. Meyer G, Doppierio S, Daffonchio L, Cremaschi D (1997) S-carbocysteine-lysine salt monohydrate and cAMP cause non-additive activation of the cystic fibrosis transmembrane regulator channel in human respiratory epithelium. FEBS Lett 404:11–14
31. Nakahari T, Marunaka Y (1996) Regulation of cell volume by β_2-adrenergic stimulation in rat fetal distal lung epithelial cells. J Membr Biol 151:91–100
32. Nakajima A, Morita M, Takemura A, Kamimura S, Okuno M (2005) Increase in intracellular pH induces phosphorylation of axonemal proteins for activation of flagellar motility in starfish sperm. J Exp Biol 208:4411–4418
33. Ozawa K, Tamura A, Ikeda K, Kawai E, Kondo T, Fukano Y, Nomura S, Ishihara Y, Masujima T (1997) Video-microscopy for analysis of molecular dynamics in cells. J Pharm Biomed Anal 15:1483–1488
34. Peitzmann ER, Zaidman NA, Maniak PJ, O'Grady SM (2016) Carvedilol binding to β_2-adrenergic receptors inhibits CFTR-dependent anion secretion in airway epithelial cells. Am J Physiol Lung Cell Mol Physiol 310:L50–L58
35. Pier GB, Grout M, Zaidi TS (1997) Cystic fibrosis transmembrane conductance regulator is an epithelial cell receptor for clearance of Pseudomonas aeruginosa from the lung. Proc Natl Acad Sci U S A 94:12088–12093
36. Rogers DF (2007) Mucoactive agents for airway mucus hypersecretory diseases. Respirr Care 52:1176–1193
37. Salathe M (2007) Regulation of mammalian ciliary beating. Annu Rev Physiol 69:401–422
38. Shiima-Kinoshita C, Min KY, Hanafusa T, Mori H, Nakahari T (2004) β_2-adrenergic regulation of ciliary beat frequency in rat bronchiolar epithelium: potentiation by isosmotic cell shrinkage. J Physiol 554:403–416
39. Shimamoto C, Umegaki E, Katsu K, Kato M, Fujiwara S, Kubota T, Nakahari T (2007) $[Cl^-]_i$ modulation of Ca^{2+}-regulated exocytosis in ACh-stimulated antral mucous cells of guinea pig. Am J Physiol Gastrointest Liver Physiol 293:G824–G837
40. Shiozaki A, Miyazaki H, Niisato N, Nakahari T, Iwasaki Y, Itoi H, Ueda Y, Yamagishi H, Marunaka Y (2006) Furosemide, a blocker of $Na^+/K^+/2Cl^-$ cotransporter, diminishes proliferation of poorly differentiated human gastric cancer cells by affecting G_0/G_1 state. J Physiol Sci 56:401–406
41. Shpetner HS, Paschal BM, Vallee RB (1988) Characterization of the microtubule-activated ATPase of brain cytoplasmic dynein (MAP 1C). J Cell Biol 107:1001–1009
42. Sutto Z, Conner GE, Salathe M (2004) Regulation of human airway ciliary beat frequency by intracellular pH. J Physiol 560:519–532
43. Tohda H, Foskett JK, O'Brodovich H, Marunaka Y (1994) Cl^- regulation of a Ca^{2+}-activated nonselective cation channel in β-agonist-treated fetal distal lung epithelium. Am J Physiol Cell Physiol 266:C104–C109
44. Tokuda S, Shimamoto C, Yoshida H, Murao H, Kishima G, Ito S, Kubota T, Hanafusa T, Sugimoto T, Niisato N, Marunaka Y, Nakahari T (2007) HCO_3^--dependent pH_i recovery and overacidification induced by NH_4^+ pulse in rat lung alveolar type II cells: HCO_3^--dependent NH_3 excretion from lungs? Pflügers Arch Eur J Physiol 455:223–239
45. Treharne KJ, Marshall LJ, Mehta A (1994) A novel chloride-dependent GTP-utilizing protein kinase in plasma membranes from human respiratory epithelium. Am J Physiol (Lung Cell Mol Physiol 11) 267:L592–L601
46. Wang L, Shen M, Guo X, Wang B, Xia Y, Wang N, Zhang Q, Jia L, Wang X (2017) Volume-sensitive outwardly rectifying chloride channel blockers protect against high glucose-induced apoptosis of cardiomyocytes via autophagy activation. Sci Rep 7:44265. https://doi.org/10.1038/srep44262
47. Wang YY, Lin YH, Wu YN, Chen YL, Lin YC, Cheng CY, Chiang HS (2017) Loss of SLC9A3 decreases CFTR protein and causes obstructed azoospermia in mice. PLoS Genet 13:e1006715. https://doi.org/10.1371/journalpgen.1006715
48. Wanner A, Salathe M, O'riordan TG (1996) Mucociliary clearance in the airways. Am J Respir Crit Care Med 154:1968–1902

49. Xu WM, Shi QX, Chen WY, Zhou CX, Ni Y, Rowlands DK, Liu GY, Zhu H, Ma ZG, Wang XF, Chen ZH, Zhou SC, Dong HS, Zhang XH, Chung YW, Yuan YY, Yang WX, Chan HC (2007) Cystic fibrosis transmembrane conductance regulator is vital to sperm fertilizing capacity and male fertility. Proc Natl Acad Sci U S A 104:9816–9821
50. Yaghi A, Dolovich MB (2016) Airway epithelial cell cilia and obstructive lung disease. Cells 5(4):E40